Prediction of one-dimensional CrN nanostructure as a promising ferromagnetic half-metal

Wenyu Xiang(相文雨)[1], Yaping Wang(王亚萍)[2], Weixiao Ji(纪维霄)[1], Wenjie Hou(侯文杰)[3], Shengshi Li(李胜世)[1,†], and Peiji Wang(王培吉)[1]

[1] *Spintronics Institute, School of Physics and Technology, University of Jinan, Jinan* 250022, *China*
[2] *State Key Laboratory of Crystal Materials and Institute of Crystal Materials, Shandong University, Jinan* 250100, *China*
[3] *School of Computer Science and Technology, Northwestern Polytechnical University, Xi'an* 710129, *China*

(Received 19 September 2022; revised manuscript received 23 December 2022; accepted manuscript online 11 January 2023)

Searching for one-dimensional (1D) nanostructure with ferromagnetic (FM) half-metallicity is of significance for the development of miniature spintronic devices. Here, based on the first-principles calculations, we propose that the 1D CrN nanostructure is a FM half-metal, which can generate the fully spin-polarized current. The *ab initio* molecular dynamic simulation and the phonon spectrum calculation demonstrate that the 1D CrN nanostructure is thermodynamically stable. The partially occupied Cr-d orbitals endow the nanostructure with FM half-metallicity, in which the half-metallic gap (Δs) reaches up to 1.58 eV. The ferromagnetism in the nanostructure is attributed to the superexchange interaction between the magnetic Cr atoms, and a sizable magnetocrystalline anisotropy energy (MAE) is obtained. Moreover, the transverse stretching of nanostructure can effectively modulate Δs and MAE, accompanied by the preservation of half-metallicity. A nanocable is designed by encapsulating the CrN nanostructure with a BN nanotube, and the intriguing magnetic and electronic properties of the nanostructure are retained. These novel characteristics render the 1D CrN nanostructure as a compelling candidate for exploiting high-performance spintronic devices.

Keywords: half-metal, ferromagnetism, one-dimensional nanostructure, first-principles calculations

PACS: 71.15.Mb, 73.22.–f, 75.75.–c **DOI:** 10.1088/1674-1056/acb200

1. Introduction

Spintronics, as one of the important research fields in the modern condensed matter physics, has sparked great interest in recent decades.[1] The purpose of spintronics is to utilize the spin degrees of freedom of electrons to storage, transport and process information, and to develop the electronics with advantages of nonvolatility, high-speed processing and low energy consumption.[2] Exploring magnetic material with high spin-polarization ratio and room-temperature magnetic order is a very significant aspect for the spintronic research. Among various magnetic materials, half-metallic magnet has received widespread attention due to the 100% spin-polarization ratio at the Fermi level (E_F), which is deemed as a promising candidate for spintronic applications.[3,4] This kind of material is featured with a metallic nature for one spin channel and an insulating nature for the opposite spin channel, and thus the fully spin-polarized current is expected to be produced. In view of this unique characteristic, half-metal can be used to design efficient spin filter. The half-metallicity was first discovered in Heusler alloys,[5] and subsequently demonstrated in other materials, such as manganese perovskites and metal-DNA complexes.[6,7] Recently, as the rise of two-dimensional (2D) materials, great efforts had been devoted to exploiting half-metallicity in 2D systems. Various 2D materials were predicted to possess intrinsic half-metallicity, including iron dihalide,[8] transition-metal (TM) dihydride,[9] TM dinitride,[10] and Cr_3X_4 (X = S, Se, Te).[11] Besides, the half-metallicity is also achievable by external strategies, such as chemical functionalization, carrier doping and external electric field.[12–17] As a matter of fact, from the perspective of scaling down of spintronic devices, exploring one-dimensional (1D) half-metallic nanostructure is more desirable.

Over the past decades, 1D materials had attracted considerable attention because of the exotic physical phenomena and potential application in the fields of electronics, magnetism, photonics, energy, etc.[18] To date, with the advance of nanotechnology, freestanding magnetic 1D nanostructures with well-defined diameters, compositions, length and phase purity can be successfully fabricated in experiment.[19,20] However, the anticipated half-metallicity is seldom reported, which is probably due to the presence of defects and surface passivation for nanostructures. To address this challenge, plenty of 1D half-metallic nanostructures were proposed theoretically,[21–24] whereas the scarcity of related experimental basis hinders their preparation and application. In this context, it is of significance to seek 1D half-metallic nanostructure with experimental feasibility.

Recently, 1D phosphorus nanostructures were fabricated and observed inside the carbon nanotube,[25] which provides an opportunity to obtain 1D nanostructures composed of TM and group-V elements. Once there are unpaired electrons in

†Corresponding author. E-mail: sdy_liss@ujn.edu.cn

© 2023 Chinese Physical Society and IOP Publishing Ltd

TM atoms, the magnetic coupling and half-metallicity are expected to be realized in the nanostructure. In this work, we find that the 1D CrN nanostructure is a ferromagnetic (FM) half-metal via the first-principles calculations. According to the *ab initio* molecular dynamic (AIMD) simulation and the phonon spectrum calculation, the nanostructure shows an excellent ambient stability. The half-metallicity is derived from the partially occupied Cr-d orbitals, and the superexchange interaction between Cr atoms is responsible for the FM ground state. The half-metallic gap is found to be 1.58 eV, which is large enough to prevent the spin-flip transition, and it can be effectively manipulated by the transverse stretching. The calculation of transport property indicates that the nanostructure can produce a 100% spin-polarized current. Furthermore, the half-metallic behavior is also accessible in the nanocable which is constructed based on the CrN nanostructure and BN nanotube. Our study provides a promising candidate for designing low-dimensional spintronic devices.

2. Computational methods

Our calculations were performed using the Vienna *ab initio* simulation package (VASP),[26,27] which is based on density functional theory (DFT) with a plane-wave basis set and the projector augmented wave (PAW) method.[28] The exchange–correlation interaction was described by the general gradient approximation (GGA) in the form of the Perdew–Burke–Ernzerhof (PBE) functional.[29,30] The plane wave basis was set to a cutoff energy of 400 eV. The geometric structure was fully relaxed until the energy and forces were converged to 10^{-6} eV and 0.001 eV/Å, respectively. The Brillouin zone was sampled by using a k-point mesh of $15 \times 1 \times 1$. A vacuum thickness of 20 Å was employed along b and c directions to avoid the interaction between the periodic images. To treat the localized d orbitals, the effective Hubbard U correction was adopted for the Cr atom with $U_{\text{eff}} =$ 3.5 eV.[31] The Heyd–Scuseria–Ernzerhof hybrid (HSE06) functional was used to obtain more accurate band structure.[32] The phonon spectrum was calculated using a finite displacement approach as implemented in the PHONOPY code.[33] The DFT-D3 method was taken into account to describe the van der Waals interaction in the nanocable.[34,35] The calculation of transport property was performed using the OpenMX code.[36,37]

3. Results and discussion

The geometric structure of the 1D CrN nanostructure is presented in Fig. 1(a). It shows that four Cr atoms and four N atoms are alternately connecting in a unit cell. A regular hexahedron configuration is formed with eight atoms as the vertices. The N atom works as a bridge ligand that connects neighboring four Cr atoms. This structural feature is distinctly different from that of 1D binary-V materials.[25] After structural optimization, the lattice constant and Cr–N bond length are found to be 3.97 Å and 2.00 Å, respectively. The Cr–N–Cr bond angle turns out to be 90°.

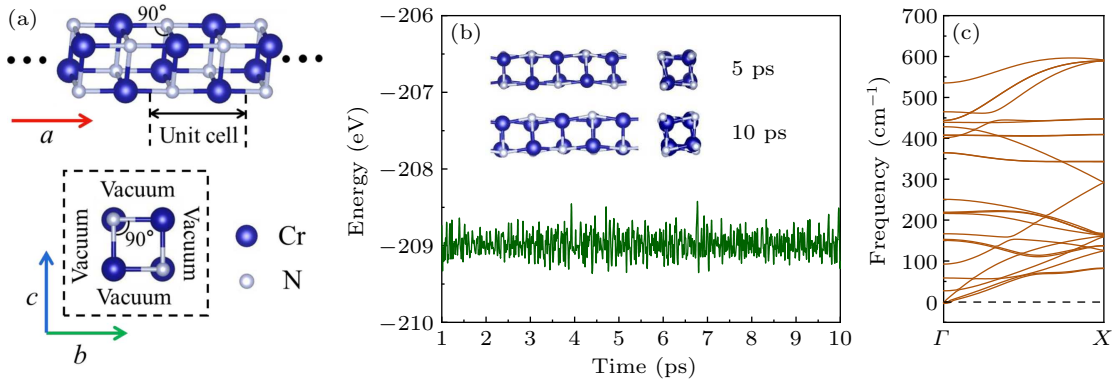


Fig. 1. (a) Structural schematic diagram of the 1D CrN nanostructure. The nanostructure is periodic in the a direction. The vacuum exists in both b and c directions, so the nanostructure is in atomic scale in both b and c directions. (b) Variation of energy as a function of time at 300 K obtained from the AIMD simulation for the CrN nanostructure. The insets are the snapshots of the nanostructure at times of 5 ps and 10 ps. (c) Phonon spectrum of the CrN nanostructure.

Then the structural stability of the 1D CrN is investigated. We first calculate the formation energy, which is defined as $E_{\text{form}} = (E_{\text{CrN}} - 4\mu_{\text{Cr}} - 4\mu_{\text{N}})/8$. Here, E_{CrN} is the total energy of CrN unit cell, while μ_{Cr} and μ_{N} are chemical potentials of Cr and N atoms using bulk chromium and nitrogen molecules, which are calculated to be -8.06 eV and -5.70 eV, respectively. The obtained E_{form} is -0.57 eV/atom, which reveals the preference of forming the CrN nanostructure rather than the pure Cr and N phases. Additionally, the cohesive energy is also calculated by the formula of $E_{\text{coh}} = (E_{\text{CrN}} - 4E_{\text{Cr}} - 4E_{\text{N}})/8$, where E_{Cr} (-3.11 eV) and E_{N} (-4.70 eV) are the energies of isolated Cr and N atoms, respectively. The E_{coh} is evaluated to be -3.55 eV/atom, suggesting that such 1D nanostructure is expected to be fabricated in experiments. Therefore, the 1D CrN nanostructure shows a favorable stability in energy. The thermodynamic stability of CrN nanos-

tructure is examined by the AIMD simulation and the phonon spectrum calculation. The AIMD simulation is performed by using a $3 \times 3 \times 1$ supercell at the temperature of 300 K. As shown in Fig. 1(b), the total energy vibrates smoothly after 1 ps preheating, and no evident structural deformation or phase transformation can be observed for the nanostructure, indicating that the 1D CrN is thermally stable. Figure 1(c) presents the calculated phonon spectrum. The absence of imaginary vibrational frequency over the entire Brillouin zone further validates the dynamic stability of the nanostructure. Such excellent structural stability, which may be attributed to unique regular hexahedron configuration, endows the CrN nanostructure with great potential for room-temperature applications.

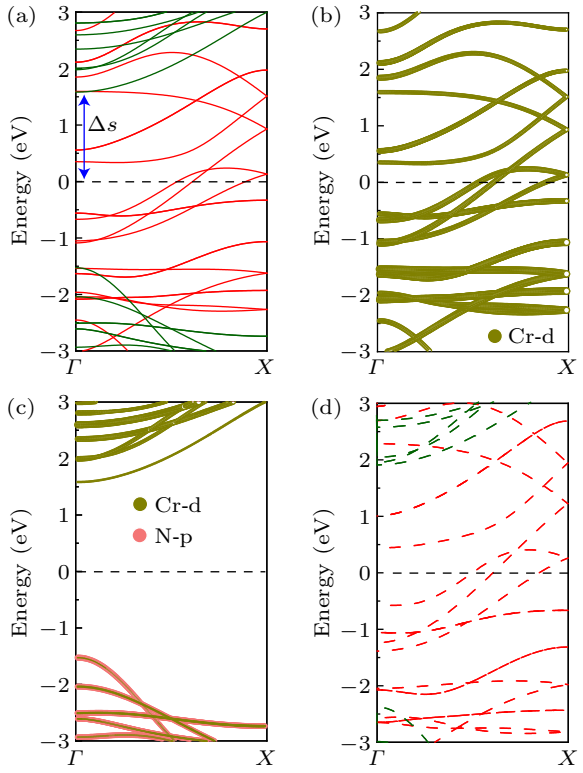


Fig. 2. (a) Spin-resolved band structure of the CrN nanostructure. The red and green lines represent the spin-up and spin-down states, respectively. (b) and (c) Orbital-resolved band structures for the spin-up and spin-down channels. (d) Spin-resolved band structure of the nanostructure calculated with HSE06 functional.

Having established the structural stability, we further explore the electronic property of the CrN nanostructure. The spin-resolved band structure is presented in Fig. 2(a). It can be observed that the spin-up and spin-down states are non-degenerate. The E_F passes through the energy bands in the spin-up channel, leading to a metallic property, whereas a semiconducting nature is obtained for the spin-down channel. Therefore, the 1D CrN belongs to a typical half-metal, characterized by the 100% spin-polarization ratio at the E_F. For a half-metal material, the half-metallic gap (Δs) is a very important parameter that determines the robustness of half-metallic character against ambient temperature. Here, Δs is deduced from the energy difference between conduction band minimum (CBM) and E_F in the spin-down channel. Notably, in VASP calculation, the E_F of a metallic system is determined by the highest energy level occupied by electrons, and the E_F of CrN nanostructure is calculated to be -3.28 eV. It is noteworthy that the Δs of the CrN nanostructure is as large as 1.58 eV, which can effectively prohibit the spin-flip transition in the system. According to the orbital-resolved band structure in Figs. 2(b) and 2(c), for the spin-up channel, the electronic states that contribute to the half-metallicity are mainly originated from the partially occupied Cr-d orbitals. On the other hand, the valence band maximum (VBM) and CBM in the spin-down channel are dominated by the N-p and Cr-d orbitals, respectively. It is well known that the electronic property of TM based compound is closely relevant to the correlation effect. To confirm the robustness of the half-metallicity in the CrN nanostructure, we further perform the band structure calculation with the U_{eff} varying from 0 eV to 5.0 eV, see Fig. S1. When the correlation effect is excluded ($U_{eff} = 0$ eV), the nanostructure exhibits a FM metallic character, in which both spin-up and spin-down states are intersected with the E_F. Interestingly, the expectant half-metallicity would emerge when the U_{eff} is larger than 1.0 eV. As a result, the half-metallicity in the CrN nanostructure shows a favorable robustness against the correlation effect. Besides, the half-metallicity is further verified by the more accurate HSE06 hybrid functional. It is found from Fig. 2(d) that the electronic behavior obtained by the HSE06 functional is consistent with that given by the GGA + U method, in which the half-metallicity is preserved, accompanied by the Δs increased to 1.91 eV.

Next, we explore the magnetic property of the CrN nanostructure. To determine the magnetic ground state, we consider one FM configuration, one nonmagnetic (NM) configuration, and four antiferromagnetic (AFM) configurations based on a $2 \times 1 \times 1$ supercell, as shown in Figs. S2(a)–S2(f). By comparing the energy between them, it is found that the FM configuration is the most energetically stable, implying that the nanostructure favors the FM coupling. The preference of FM coupling can be understood by the Cr–N–Cr superexchange interaction. In the light of the Goodenough–Kanamori–Anderson (GKA) rules,[38–40] the system with cation–anion–cation bond angle of 90° indeed often prefers the FM coupling. As mentioned above, the Cr–N–Cr bond angles are 90°, and thus the CrN nanostructure shows the FM ground state. Besides, the nanostructure has an integer magnetic moment of 12 μ_B/unit cell, in which the local magnetic moment of Cr atom is found to be about 3.0 μ_B. It means that the spin-polarized state is mainly contributed by the Cr atoms, which can be further manifested by the spin charge distribution in Fig. S2(g). Considering that the valence electron configuration of Cr atom is $3d^5 4s^1$, three electrons would be transferred from Cr atom to

neighboring N atoms when forming the CrN nanostructure, and thus the Cr^{3+} with the electron configuration of $3d^3$ is generated, which is consistent with the magnetic moment of 3.0 μ_B on each Cr atom.

As is well known, the magnetocrystalline anisotropy energy (MAE) is an important parameter for the application of magnetic material, which is responsible for the stabilities of magnetic ordering and data storage. Here, by incorporating the spin–orbit coupling (SOC) effect, the calculations of MAE with magnetization orientation along (100), (010), (001), (110), (011), and (111) directions are performed, as summarized in Table 1. It is found that the MAE is zero in the *bc* plane, indicating that the CrN exhibits an easy magnetization plane which is perpendicular to the *a* axis. In other words, the magnetization can rotate in the *bc* plane without energy consumption. The result also shows that the MAE is anisotropic in the *ac*/*ab* plane. To confirm this, Fig. 3(a) presents the angular dependence of MAE. One can see that the MAE is strongly dependent on the magnetization orientation, and the MAE reaches a maximum of 0.40 meV/unit cell when the magnetization is along the *a* axis. To give insight into the origin of magnetic anisotropy, we plot the atom- and orbital-resolved MAE in Figs. 3(b) and 3(c). One can see that the Cr atoms contribute the most to the MAE, while the contribution of N atoms is very small. The MAE is mainly arisen from the Cr-d orbitals hybridization. The hybridizations between d_{yz} and $d_{x^2-y^2}$ orbitals, d_{xy} and d_{xy} orbitals as well as d_{yz} and d_{z^2} orbitals result in the in-plane (*bc* plane) magnetic anisotropy, while the hybridizations between d_{xy} and $d_{x^2-y^2}$ orbitals as well as d_{yz} and d_{xz} orbitals give arise to the out-of-plane (*a* axis) magnetic anisotropy. Obviously, the former is stronger than the latter, and thus the nanostructure shows an easy magnetization plane. For the 1D FM nanostructure with an easy magnetization plane perpendicular to the periodic direction, it is possible to form the spin spiral state. To examine this, specific angles are introduced artificially between the magnetization orientations for two layers of Cr atoms along the *a* axis. After self-consistent calculation, the magnetization orientations of Cr atoms become parallel finally, without forming the spin spiral state. According to the Mermin–Wagner theorem,[41] long-range magnetic ordering is prohibited in the 1D isotropic Heisenberg model at finite temperature. However, the FM ordering and the half-metallicity in the 1D CrN are still promising to be realized and utilized by applying an external magnetic field or depositing the nanostructure on a FM substrate.

Table 1. Summary of MAE in meV/unit cell for the 1D CrN nanostructure with magnetization along specific directions.

(100)	(010)	(001)	(110)	(011)	(111)
0.40	0.00	0.00	0.24	0.00	0.10

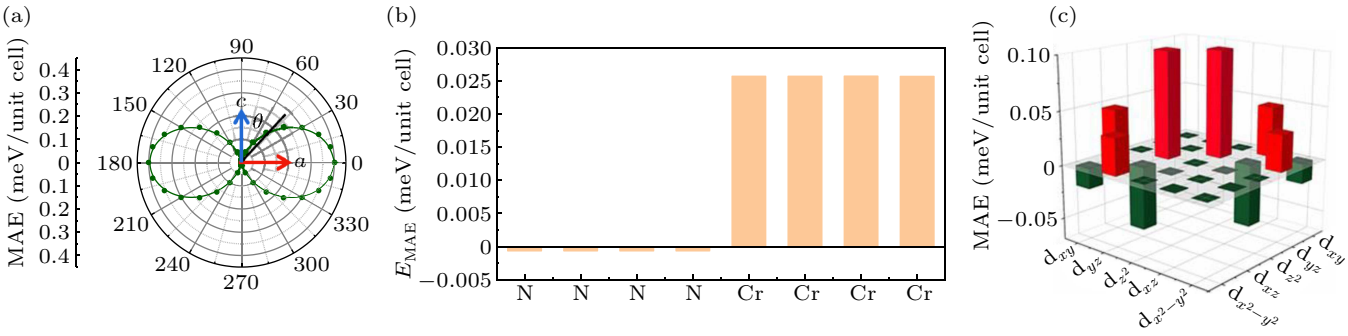


Fig. 3. (a) Angular dependence of MAE for the CrN nanostructure. (b) Atom-resolved MAE of the CrN nanostructure. (c) MAE contribution from the Cr-d orbitals hybridization.

Then the transport property of the CrN nanostructure is discussed by calculating the current–voltage (*I*–*V*) curve with the combination of first-principle and nonequilibrium Green's function methods. The spin-resolved *I*–*V* curve is plotted in Fig. 4(a). It shows that only the spin-up channel can produce the current, whereas the current of the spin-down channel is equal to zero, implying that the current in the 1D CrN is 100% spin-polarized. More interestingly, the characteristic of negative differential resistance (NDR)[42–44] can be observed when the voltage is larger than 1.0 V. By analyzing the transmission spectra in Figs. 4(b) and 4(c), we find that with the increase of bias voltage, although the bias energy window becomes wider, the transmission inside the window is suppressed, which directly results in the occurrence of NDR phenomenon.[45,46] Such spin-polarized NDR effect may be potentially valuable in practical application.

Furthermore, we have investigated the effect of transverse stretching on the electronic and magnetic properties of the 1D CrN. To figure out the change of MAE, the energy difference between the magnetization along the (100) and (001) directions is calculated, which is defined as $E_{MAE} = E_{100} - E_{001}$. Figure 5(a) displays the variations of Δs and E_{MAE} as a function of the length of nanostructure. It is found that the Δs is enhanced with increasing length of nanostructure. With the transverse stretching of nanostructure, the Cr–N bond length in the *a* direction is enlarged, and thus the hybridization be-

tween Cr-d and N-p orbitals becomes weakened, which makes electronic states more localized. Thereby, the CBM in the spin-down channel shifts to higher energy, rendering the enhancement of Δs. To make it more understandable, the partial charge densities of the CBM in the spin-down channel for the nanostructure under different degrees of stretching are plotted in Fig. S3, in which the hybridization between transverse Cr and N atoms is significantly suppressed with increasing stretching. Moreover, the E_{MAE} is diminished as the nanostructure is stretched. Taking the nanostructure whose unit cell length is 4.20 Å as a representative, we plot the orbital-resolved MAE of Cr atom, as shown in Fig. 5(b). It shows that the d_{yz} and $d_{x^2-y^2}$ hybridization as well as the d_{yz} and d_{z^2} hybridization are reduced sharply, whereas the d_{xy} and d_{xy} hybridization is increased. Overall, the d-orbitals hybridization that contributes to the in-plane (*bc* plane) magnetization is decreased. Meanwhile, the d_{xy} and $d_{x^2-y^2}$ hybridization as well as the d_{yz} and d_{xz} hybridization are enhanced slightly. The combination of these two phenomena ultimately leads to the decrease of E_{MAE}. Additionally, it is important to note that the half-metallicity, FM ground state and magnetic moment of the 1D CrN are persisted during the whole transverse stretching.

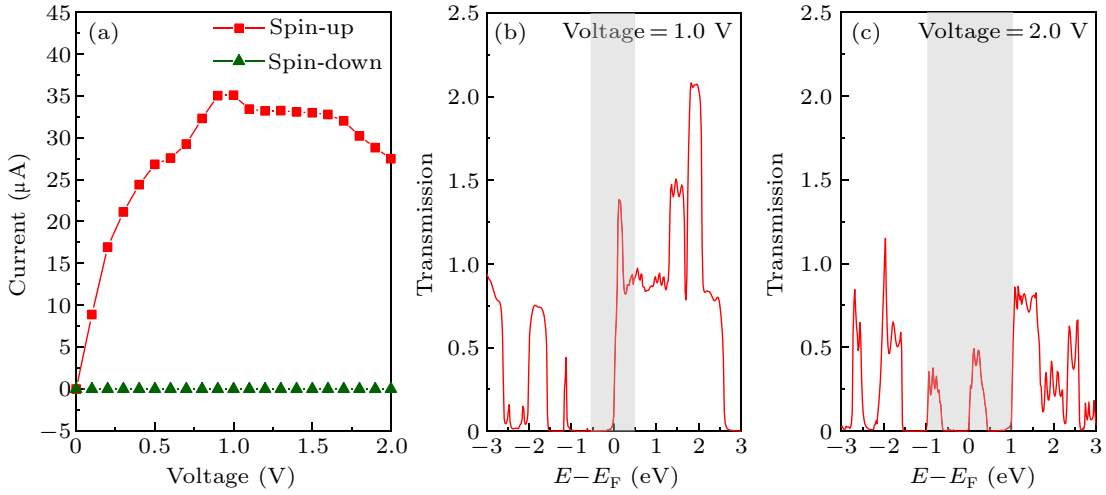


Fig. 4. (a) Calculated spin-resolved *I*–*V* curve of the CrN nanostructure in the *a* direction. (b) and (c) Transmission spectra of the CrN nanostructure with the voltages of 1.0 V and 2.0 V, respectively. The transport property is contributed by the states in the bias energy windows, which are marked as the shadow areas.

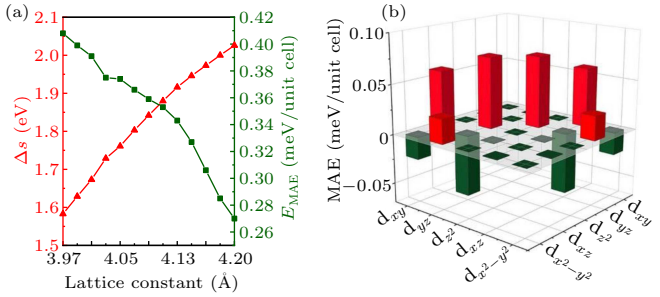


Fig. 5. (a) Variations of Δs and E_{MAE} with the increase of unit cell length. (b) MAE contribution from the Cr-d orbitals hybridization for the nanostructure whose unit cell length is 4.20 Å.

To utilize a 1D material as the active element in electronic devices, it is essential to protect its structural, magnetic and electronic properties from ambient environment. The design of nanocable by wrapping an insulating outer sheath on the 1D material provides a feasible strategy to deal with above issue. Based on this concept, we construct a nanocable by using a $1 \times 1 \times 1$ CrN and a $1 \times 1 \times 1$ (11,0) BN zigzag nanotube, as depicted in Fig. 6(a), in which the lattice mismatch between them is 6.5%. The nearest distance between the CrN nanostructure and BN nanotube is about 2.90 Å, which is large enough to avoid forming the hybridization. After structural optimization, the 1D CrN maintains its pristine structure in the nanocable. The spin-resolved band structure of the nanocable is presented in Fig. 6(b). The spin-up and spin-down channels also exhibit the metallic and semiconducting properties, respectively, which testifies the presence of half-metallicity in the nanocable. By projecting the components contribution on the energy bands, the electronic states at the E_{F} in the spin-up channel are dominated by the CrN nanostructure. Hence, the half-metallicity of CrN is preserved intactly and unaffected by the BN nanotube.

Experimentally, the highly crystalline CrN ultrathin films have been reported.[47–52] Although both of predicted CrN nanostructure in this article and CrN film belong to chromium nitride, there are fundamental difference between them. Firstly, in terms of dimension, the former and latter are 1D and 2D materials, respectively. Besides, the bonding mode between Cr and N atoms are different in these two materials. The Cr atom in the former and latter are four-coordinated and six-coordinated, respectively. In this context, distinct orbital hybridizations are generated, which lead to various magnetic and electronic properties for these two materials. Generally, the CrN film favors AFM coupling and shows thickness dependent metal-to-insulator transition.[48–50] However, as mentioned above, the proposed 1D CrN nanostructure is FM, and

it is intrinsically conductive, which can generate the fully spin-polarized current.

Having identified the unique magnetic and electronic properties of the CrN nanostructure, we further expand our investigation to other 1D TMN (TM = Sc, Ti, V, Mn, Fe, Co, Ni, Cu, Zn) nanostructures which share a similar structure to that of CrN, to explore the possibility of realizing the half-metallicity. Figures S4–S12 display the geometric structures, magnetic ground states, phonon spectra and band structures of these TMN nanostructures. As can be seen, the magnetic ground state of TMN is strongly dependent on the selection of TM atom. The ScN and CuN nanostructures prefer the NM state. The FM ground state is demonstrated for the MnN, NiN and ZnN nanostructures, while the 1D VN, TiN, FeN and CoN exhibit the AFM ground state. Nevertheless, according to the calculated phonon spectra, only the TiN nanostructure is dynamically stable, and it belongs to a AFM semiconductor. Despite the fact that the 1D MnN and ZnN possess the half-metallicity, there are imaginary frequencies in their phonon spectra. Thus, it is challengeable to achieve the half-metallicity in these nanostructures.

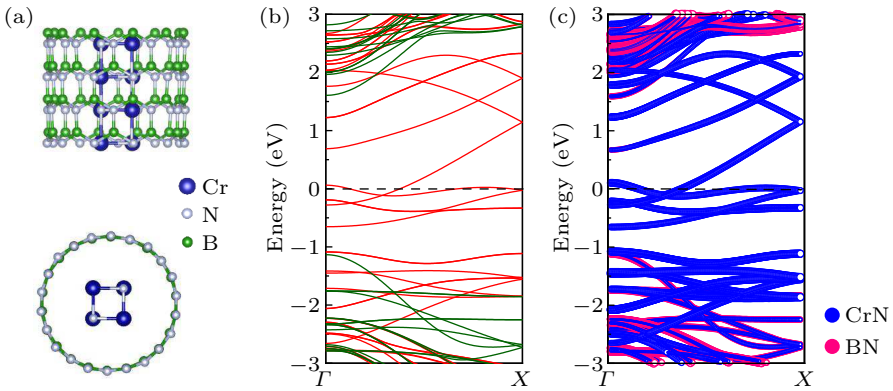


Fig. 6. (a) Geometric structure of the designed nanocable. (b) Spin-resolved band structure of the nanocable. (c) Projected band structure of the nanocable.

4. Conclusion

We have computationally predicted that the 1D CrN nanostructure is a FM half-metal with 100% spin-polarization ratio at the E_F. The comprehensive calculations of stability indicate that the nanostructure is thermodynamically stable. The half-metallicity is arisen from the partially occupied Cr-d orbitals, accompanied by a sizable Δs of 1.58 eV, and the ferromagnetism can be explained by the superexchange interaction between Cr atoms. The calculation of transport property reveals that the fully spin-polarized current is accessible in the 1D CrN. Furthermore, the half-metallicity shows a robustness against the transverse stretching, in which the Δs can be effectively modulated. When the 1D CrN is encapsulated by a BN nanotube, the FM half-metallicity of the nanostructure can be preserved intactly. Our findings greatly broaden the family of 1D half-metal materials and open a path for developing low-dimensional spintronic devices with high-performance.

Acknowledgments

Project supported by the National Natural Science Foundation of China (Grant Nos. 12004137, 62071200, and 12104236), and Shandong Provincial Natural Science Foundation of China (Grant Nos. ZR2020QA052, ZR2020ZD28, ZR2021MA040, and ZR2021MA060).

References

[1] Žutić I, Fabian J and Sarma S D 2004 *Rev. Mod. Phys.* **76** 323
[2] Fert A 2008 *Rev. Mod. Phys.* **80** 1517
[3] Pickett W E and Moodera J S 2001 *Phys. Today* **54** 39
[4] Xiang H, Yang J, Hou J G and Zhu Q 2006 *J. Am. Chem. Soc.* **128** 2310
[5] de Groot R A, Muller F M, van Engen P G and Bushow K H J 1983 *Phys. Rev. Lett.* **50** 2024
[6] Park J H, Vescovo E, Kim H J, Kwon C, Ramesh R and Venkatesan T 1998 *Nature* **392** 794
[7] Mallajosyula S S and Pati S K 2007 *J. Phys. Chem. B* **111** 13877
[8] Ashton M, Gluhovic D, Sinnott S B, Guo J, Stewart D A and Hennig R G 2017 *Nano Lett.* **17** 5251
[9] Wu Q, Zhang Y, Zhou Q, Wang J and Zeng X C 2018 *J. Phys. Chem. Lett.* **9** 4260
[10] Liu Z, Liu J and Zhao J 2017 *Nano Res.* **10** 1977
[11] Zhang X, Wang B, Guo Y, Zhang Y, Chen Y and Wang J 2019 *Nanoscale Horiz.* **4** 859
[12] Kan E, Li Z, Yang J and Hou J G 2008 *J. Am. Chem. Soc.* **130** 4224
[13] Dutta S, Manna A K and Pati S K 2009 *Phys. Rev. Lett.* **102** 096601
[14] Cao T, Li Z and Louie S G 2015 *Phys. Rev. Lett.* **114** 236602
[15] Jiang P, Kang L, Zheng X, Zeng Z and Sanvito S 2020 *Phys. Rev. B* **102** 195408
[16] Son Y W, Cohen M L and Louie S G 2006 *Nature* **444** 347
[17] Tang C, Zhang L, Sanvito S and Du A 2020 *J. Mater. Chem. C* **8** 7034
[18] Garnett E, Mai L and Yang P 2019 *Chem. Rev.* **119** 8955
[19] Xia Y, Yang P, Sun Y, Wu Y, Mayers B, Gates B, Yin Y, Kim F and Yan H 2003 *Adv. Mater.* **15** 353
[20] Qu Y, Arguilla M Q, Zhang Q, He X and Dinca M 2021 *J. Am. Chem. Soc.* **143** 19551
[21] Fu L, Shang C, Zhou S, Guo Y and Zhao J 2022 *Appl. Phys. Lett.* **120** 163102
[22] Li X, Lv H, Dai J, Ma L, Zeng X C, Wu X and Yang J 2017 *J. Am. Chem. Soc.* **139** 6290

[23] Kumar S, Kumawat R L and Pathak B 2019 *J. Phys. Chem. C* **123** 15717
[24] Li S S, Wang Y P, Hu S J, Chen D, Zhang C W and Yan S S 2018 *Nanoscale* **10** 15545
[25] Zhang J, Fu C, Song S, Du H, Zhao D, Huang H, Zhang L, Guan J, Zhang Y, Zhao X, Ma C, Jia C L and Tomanek D 2020 *Nano Lett.* **20** 1280
[26] Kresse G and Furthmüller J 1996 *Phys. Rev. B* **54** 11169
[27] Kresse G and Hafner J 1994 *Phys. Rev. B* **49** 14251
[28] Kresse G and Joubert D 1999 *Phys. Rev. B* **59** 1758
[29] Grimme S 2006 *J. Comput. Chem.* **27** 1787
[30] Perdew J P and Wang Y 1992 *Phys. Rev. B* **45** 13244
[31] Anisimov V I, Zaanen J and Andersen O K 1991 *Phys. Rev. B* **44** 943
[32] Heyd J, Scuseria G E and Ernzerhof M 2003 *J. Chem. Phys.* **118** 8207
[33] Togo A, Oba F and Tanaka I 2008 *Phys. Rev. B* **78** 134106
[34] Grimme S, Antony J, Ehrlich S and Krieg H 2010 *J. Chem. Phys.* **132** 154104
[35] Grimme S, Ehrlich S and Goerigk L 2011 *J. Comput. Chem.* **32** 1456
[36] Ozaki T, Nishio K and Kino H 2010 *Phys. Rev. B* **81** 035116
[37] Ozaki T 2007 *Phys. Rev. B* **75** 035123
[38] Kanamori J 1960 *J. Appl. Phys.* **31** S14
[39] Goodenough J B 1955 *Phys. Rev.* **100** 564
[40] Anderson P W 1959 *Phys. Rev.* **115** 2
[41] Mermin N D and Wagner H 1966 *Phys. Rev. Lett.* **17** 1133
[42] Chen Y C, Hsu S H, Kaun C C and Lin M T 2014 *J. Phys. Chem. C* **118** 21199
[43] Zhou B, Yang B, Ng M F, Sullivan B M, Tan B C V and Shen L 2018 *J. Am. Chem. Soc.* **130** 4023
[44] Zhu S, Fu H, Gao G, Wang S, Ni Y and Yao K 2013 *J. Chem. Phys.* **139** 024309
[45] Hu J, Xiong W, Huang P, Wang Y, Cai C and Wang J 2020 *Appl. Surf. Sci.* **528** 146957
[46] Hu Y, Li S S, Ji W X, Zhang C W, Ding M, Wang P J and Yan S S 2020 *J. Phys. Chem. Lett.* **11** 485
[47] Miyano R, Kimura K, Izumi K, Takikawa H and Sakakibara T 2000 *Vacuum* **59** 159
[48] Jin Q, Cheng H, Wang Z, *et al.* 2021 *Adv. Mater.* **33** 2005920
[49] Jin Q, Wang Z, Zhang Q, Zhao J, Cheng H, Lin S, Chen S, Chen S, Guo H, He M, Ge C, Wang C, Wang J O, Gu L, Wang S, Yang H, Jin K L and Guo E J 2021 *Phys. Rev. Mater.* **5** 023604
[50] Jin Q, Zhao J, Roldan M A, Qi W, Lin S, Chen S, Hong H, Fan Y, Rong D, Guo H, Ge C, Wang C, Wang J O, Wang S, Jin K J and Guo E J 2022 *Appl. Phys. Lett.* **120** 073103
[51] Meng C, Yang L, Wu Y, Tan J, Dang W, He X and Ma X 2019 *J. Nucl. Mater.* **515** 354
[52] Zhang M, Li M K, Kim K H and Pan F 2009 *Appl. Surf. Sci.* **255** 9200